BIOINSPIRED UNDERWATER ROBOT WITH SHAPE MEMORY METAL-BASED ACTUATORS

FAUSTO RAMIRO CABRERA AGUAYO [1]
Florida Atlantic University (FAU)
Guest Researcher,
Department of Ocean and Mechanical Engineering
fausto.cabrera@espoch.edu.ec
https://orcid.org/0000-0002-0816-155X

DIEGO RAMIRO ÑACATO ESTRELLA [2]
diego.nacato@espoch.edu.ec
Escuela Superior Politécnica de Chimborazo (ESPOCH)
Facultad de informática y electrónica
Carrera Electrónica y Automatización
https://orcid.org/0000-0002-7233-9076

FABRICIO JAVIER SANTACRUZ SULCA [3]
Escuela Superior Politécnica de Chimborazo (ESPOCH)
fabricio.santacruz@espoch.edu.ec
Facultad de informática y electrónica
Carrera Telecomunicaciones
https://orcid.org/0000-0001-7123-2552

ROBERTO ISRAEL PALACIOS PRIETO [4]
robertoi.palacios23@gmail.com
Investigador Independiente
https://orcid.org/0009-0000-4117-9594

BRYAN ALEXANDER AGUIRRE CEVALLOS [5]
aguirre.cevallos.b.a@gmail.com
Investigador Independiente
https://orcid.org/0009-0002-3483-8066

OSCAR CURET [6]
Florida Atlantic University (FAU)
Associate Professor,
Department of Ocean and Mechanical Engineering
ocuret@fau.edu
https://orcid.org/0000-0002-3202-6841

Abstract: A bio-inspired robot was implemented in a fish whose main objective is the analysis of the interaction of the pectoral and caudal fins during the two-dimensional displacement, the pectoral and caudal fins were implemented for rotation and displacement, its pectoral fin has a dimension of 30mm high and 33mm wide, It consists of two parts, its base with cavities to house the actuator and its cover to hold and compact the fin, the caudal fin is created from a mold with cavities to house the actuator with a rigid fin at the end to have a greater movement, its dimension is 91. 69mm long, 30mm wide at the beginning and 40mm wide at the end, the robot as a whole has a dimension of 249.37mm long and 92.5mm wide with a weight of 254.5g. The actuators based on nitinol shape memory metals were used, for which tests were conducted with 2 wire gauges with diameters of 0. 5mm and 1mm, the 0.5mm cable has an activation of 60±10°C and the 1mm of 40±10°C, for which it was first analyzed the force developed by each of the actuators at different temperatures obtaining the following results, the 0. 5mm when subjected to force tests with a configuration of 60°C activation temperature with a voltage of 1.25 V at 2 A manages to lift an intermediate weight in terms of our tests of 20g reaches its final set point but with a not favorable time and having small deformations in its initial engraving, the 1mm material was subjected to the same tests with a configuration of 40°C activation temperature with a voltage of 0. 54 V at 2.25 A having favorable results in terms of reaching its final set point in the desired time and without having any final deformation, for which already established the tests it is analyzed that the two arrive to lift corresponding but the material of 0. 5mm material consumes more energy with a longer time than the 1mm material, so for the displacement of the robot the 1mm material was chosen because it has the necessary force to fulfill its objective, besides not consuming energy in excess. Once analyzed it was possible to achieve the two-dimensional displacement with pectoral and flow fins, with an oscillatory movement of the rigid flow fin, and turns with the pectoral fins, with an activation of 40°C at 0.54V with 2.25A and with the 1mm actuators a speed of 3.33 m/s was obtained.

Keywords: Bio-inspired Robot, Caudal Fin, Pectoral Fin, Nitinol, Two-dimensional Displacement, Oscillating, oscillating.

1. Introduction

Underwater research has been extended in order to find solutions to problems within an aquatic ecosystem by making known the reality of this environment, as well as the development of new technologies.[1]

Underwater robots must possess the ability to propulsion and maneuver underwater, these mechanisms can be manned or unmanned. To achieve these capabilities there are propulsion systems that use an electric motor, to which a propeller is connected, when rotating the propeller produces a push effect by displacing the water from front to back, or the bioinspired fish that use as a propulsion system fins that allow a cyclic movement, producing water waves that drive the mechanism forward [2][2], [3].

Currently the research of bioinspired underwater robots focuses on copying and improving the natural locomotion of different beings that move in an underwater environment such as the robotic fish G9 developed at the University of Essex, United Kingdom that aims to reproduce the different modes of movement of a real fish according to its own criteria, To do this, they indexed different behaviors of the fish in a library, which uses a computer to generate varied and unexpected trajectories of the robot, in order to achieve a prototype that could swim like a real fish and that had an autonomous behavior. The UC-Ika 1 robot developed at the University of Canterbury, New Zealand and published in the International Journal of Advanced Robotic Systems. It is a robot bioinspired by the swimming movement of a tuna, consists of 4 degrees of freedom which generates a wave movement thanks to its pendulum and caudal fin driven by a single direct current motor.[4][5]

Most of the robots mentioned above use as a means of propulsion electric actuators which consist of a simple design, high operating speed and are readily available in the market, DC motors and servo motors are the two main types of actuators used in this category, the disadvantage of using these actuators is the noise they produce in the underwater environment, As a consequence they alter the ecosystem and aquatic life, for these reasons other propulsion systems such as intelligent actuators are proposed, these actuators have the ability to perform complex movements similar to those produced by different living beings, so they are used largely for the design of bioinspired robots, this system is continuous and simple, more similar to nature than the discreet and rigid movements that bodies present when using electric actuators.[6][7][3], [8]

Metal-based actuators with shape memory, such as those used in the creation of the flexible pectoral fin that can perform 3D movements or where they present a design of a flexible robotic fish driven by an SMA cable, can opt for different shapes according to their application, for example, opt for a straight shape and be subjected to a tension exerting large forces with small linear movements, Another example is the coil spring shape which has the characteristic of large linear movements and small forces or large rotations. Torsion bars of shape-memory metal-based actuators have large rotations and small torques.[9][10][11]

This article presents the design of a bioinspired robot using for its propulsion of metal-based actuators with shape memory which are embedded in the pair of pectoral fins and caudal fin, both rigid, in order to achieve an oscillatory movement through the tail of the robot and achieve two-dimensional displacement in a controlled environment, obtaining results such as caudal flapping for the propulsion of the robot, and turns to the right and left by the movement of the pectoral fin

2. Theoretical framework

2.1. Function of the pectoral fin.

The pair of pectoral fins are each located on one side of the fish and are used as oars on most bony fish allowing stability, braking, turns and slow propulsion of the fish.[12]

2.2. Caudal fin function.

The caudal fin is responsible for the propulsion of the fish through an underwater environment, allowing it to swim, the shape of this fin determines how a fish swims. The caudal fin that allows the propulsion of the underwater robot was inspired by the homocercal tail fin, which consists of an upper and lower lobe generally of the same size and shape. The side-to-side movement of the caudal fin allows the bioinspired underwater robot to propel itself through the water by what is called carangiform locomotion. [13]

The homocercal tail generates a reaction force directed forward because of the flexion of the vertical axis and to move symmetrically with the dorsal and ventral lobes moving in synchrony as shown in Figure 1.[13]

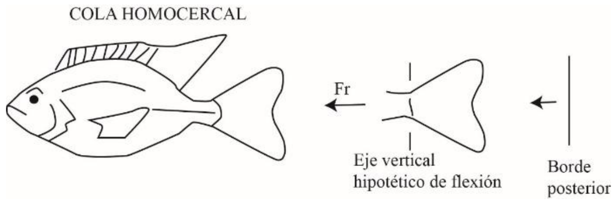

Figure 1. Homocercal tail.

2.3. Shape-memory metal-based actuators

Actuators based on metals with shape memory work under the transformation of their crystal structure into another and the reorientation of this, that is, between austenite to martensite or vice versa, as shown in figure 2. When this metal is heated, usually by passing an electric current through the SMA fiber, for which its conductive capacity is used, the martensite is transformed into austenite and the fiber contracts. A subsequent cooling of the metal converts austenite back into martensite, and the internal stresses of the metal return it partially or totally to its original form, thus achieving the movement of the actuator as the application requires.[11]

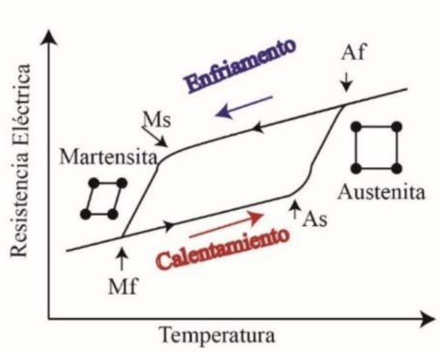

Figure 2. Shape memory metal behavior

In Figure 3. represents the behavior of the shape-memory metal-based actuator, which shows no change in its cold form above the final austenitic transformation temperature (Af) or below the final martensitic transformation temperature (Mf). When the actuator is deformed below (Mf) it remains with that deformation until it heats up. The recovery of the form begins at the starting temperature of austenitic transformation (As) and is complete at (Af), At the inflection point between As and (Af), about half of the original form is already recovered. Once the shape has recovered in (Af), there are no further shape changes when the actuator is cooled to below (Mf) and the shape memory can only be reactivated by deforming the martensite again, i.e. the shape memory effect occurs only once. [14]

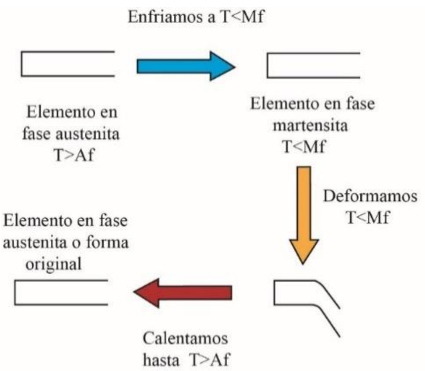

Figure 3. Behavior of the actuator based on shape memory metal

2.4. Cinematicrobot bioinspired by a fish

The kinematic model analyzed in , is applied to a robot inspired bio fish driven by caudal fin with 1 GDL,[15] where a mathematical model was developed taking as reference certain angles and parameters of the system to find the desired positions and orientations of the elements as observed in equation 1 and 2, the mathematical model described below began with an approach as observed in equation 5 to obtain the final position based on the movement of each of the links of the prototype, to then obtain the direct differential kinematics in equation 12 of the prototype driven by the caudal fin of a degree of freedom.[15]

$$x1 = l1cosq1 \qquad \dot{x}1 = -\dot{l}1\dot{q}1sinq1 \tag{1}$$

$$y1 = l2sinq1 \qquad \dot{y}1 = -\dot{l}2\dot{q}1cosq1 \tag{2}$$

$$\frac{\partial x2}{\partial q2} = -l2\dot{q}2\sin\,(q1 + q2) \tag{3}$$

$$\frac{\partial y2}{\partial q2} = -l2\dot{q}2\cos\,(q1 + q2) \tag{4}$$

$$J^2v = \begin{bmatrix} -l1sinq1 & -\,l2\sin(q1+q2) & -\,l2\sin\,(q1+q2) \\ l1cosq1 & +\,l2cos(q1+q2) & +\,l2cos(q1+q2) \end{bmatrix} \begin{bmatrix} \dot{q}1 \\ \dot{q}2 \\ 0 \end{bmatrix} \tag{5}$$

$$M1J^1v^TJ^1v \tag{6}$$

$$M1 = \begin{bmatrix} -l1sinq1 & l1cosq1 & 0 \\ 0 & 0 & 0 \end{bmatrix} \begin{bmatrix} -l1sinq1 & 0 \\ l1cosq1 & 0 \\ 0 & 0 \end{bmatrix} \tag{7}$$

$$M1 = \begin{bmatrix} M1l1^2 & 0 \\ 0 & 0 \end{bmatrix} \tag{8}$$

$$J^1W^TR1 \tag{9}$$

$$\begin{bmatrix} 0 & 0 & 1 \\ 0 & 0 & 0 \end{bmatrix} \begin{bmatrix} c1 & -\,s1 & 0 \\ s1 & c1 & 0 \\ 0 & 0 & 1 \end{bmatrix} = \begin{bmatrix} 0 & 0 & 1 \\ 0 & 0 & 0 \end{bmatrix} \tag{10}$$

$$R^TJ^1W \tag{11}$$

$$\begin{bmatrix} c1 & s1 & 0 \\ -\,s1 & c1 & 0 \\ 0 & 0 & 1 \end{bmatrix} \begin{bmatrix} 0 & 0 \\ 0 & 0 \\ 1 & 0 \end{bmatrix} = \begin{bmatrix} 0 & 0 \\ 0 & 0 \\ 1 & 0 \end{bmatrix} \tag{12}$$

2.5. Dinámica de robot bioinspired em un pez

The dynamics of the bioinspired robot are represented by means of a mathematical model that relates the contact forces with the actuation and the acceleration with the trajectory of the movement. Equation 13 represents motion in a general way.[7][7]

$$T - D = Ma \tag{13}$$

Equation 14 represents the dynamic motion of the bioinspired robot obtained by the Lagrange-Euler formulation. [7]

$$\frac{dy}{dt}\left(\frac{\partial \mathcal{L}}{\partial \dot{q}_\iota}\right) - \frac{\partial \mathcal{L}}{\partial \dot{q}_\iota} = \tau_i, i = 1,2,\dots,n. \tag{14}$$

$$\mathcal{L} = K_E - P_E \tag{15}$$

Equation 14 and 15 represent the Lagrange function where it represents the number of articulation acting on the head of the bioinspired robot.τ_i[7].

3. Methodological framework

3.1. Recording and actuator activation

To obtain the movement of the bioinspired robot, etching and activation tests were carried out for which we consider the angle of attack that the robot must have to comply with its displacement, so the tests were carried out to obtain favorable results of engraving and activation, the angles of attack considered are 60°, 90° and 120°.

A graphical analysis is contemplated to identify the results, its data are taken from a set of samples which were considered taking into account aspects such as voltage, amperage, time, diameter, length and angle of attack.

The batteries used for the tests are 1S (7.4V to 300mAh), 2S (11.1V to 800mAh), 3S (14.4V to 650mAh0) and a 12V to 10A power supply.

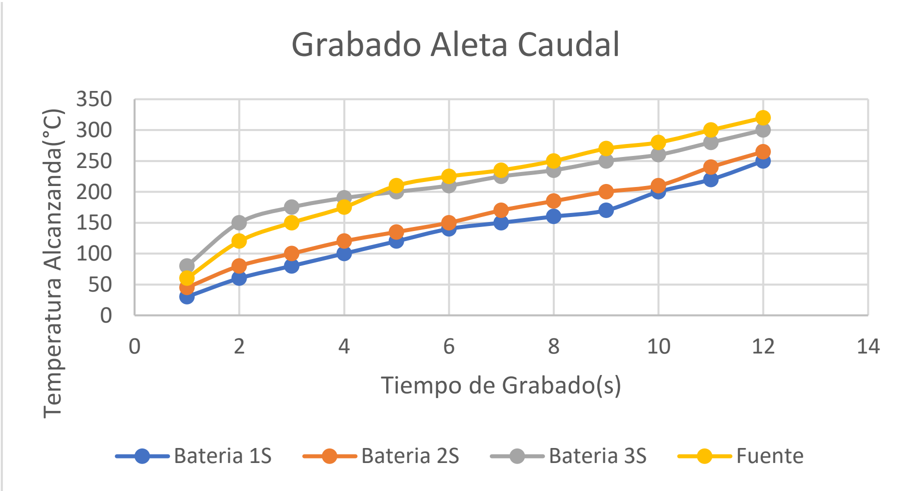

Figure 4. Engraving of the actuator used for the caudal fin.

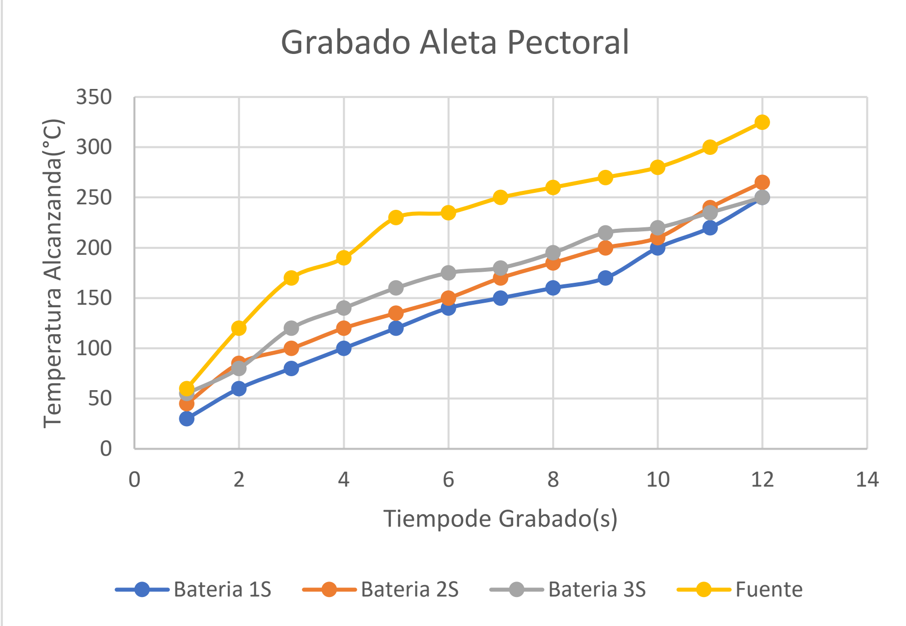

Figure 5. Engraving of the actuator used for the pectoral fin.

In the etching of the actuator used for the caudal and pectoral fin there are several power supplies which, by varying their voltage and amperage, reach a certain temperature taking into account external parameters such as time, ambient temperature, diameter and length of the actuator cable and power.

Figures 4 and 5 show us the trajectory of the temperature reached by the actuator with the different energy sources, which have different characteristics in terms of amperage, voltage, charging and discharging time, when analyzing the points of graph 1 and 2 of the caudal fin, and pectoral in relation to time and temperature, Considering that the nitinol cable has a diameter of 1mm for the two caudal and pectoral actuators, with a length of 110mm and 60mm respectively, it was analyzed in an experimental way that an acceptable range of etching taking into account the angle of attack is for the caudal and pectoral fin. $210 \pm 10\ °C$

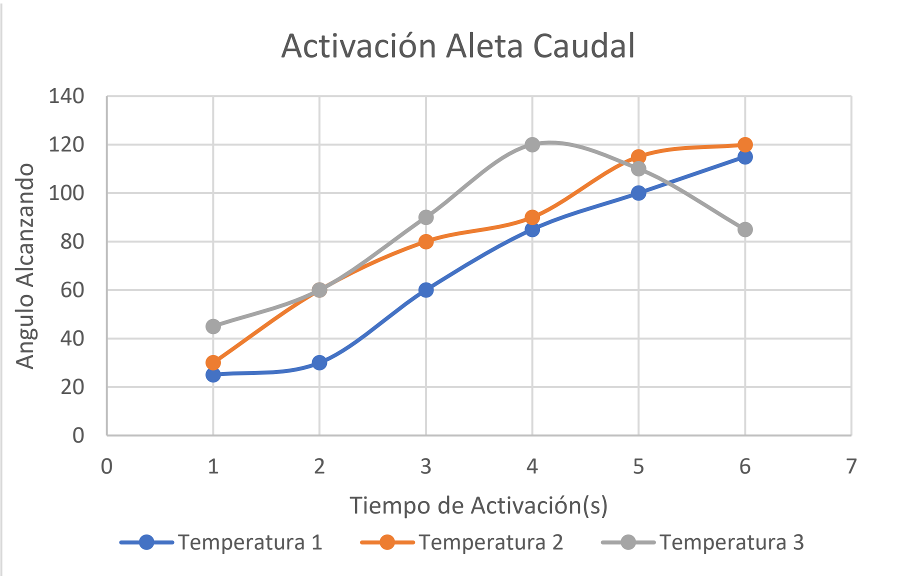

Figure 6. Activation temperature for the caudal fin actuator.

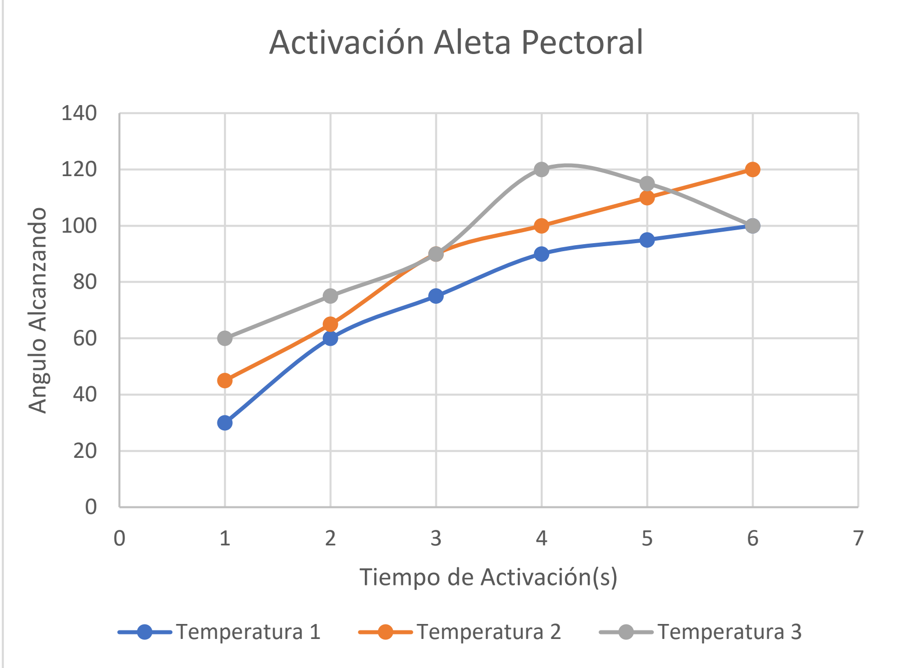

Figure 7. Activation temperature for the pectoral fin actuator.

Once the engraving has been made with the previously selected temperature, the actuator is activated for which the manufacturer gives us a range of 1mm diameter for the wire, this temperature being in ideal conditions, based on the trial and error method, we proceed with different temperatures inside and outside the mentioned range. $40 \pm 10°C$

In figures 6 and 7 as in the previous figures of engraving shows us the temperature trajectory that are generated with the different sources, the activation in the actuators depends a lot on their external parameters such as lengths, diameters and heat dissipation conditions in this case it will be subjected to immersion so water is a dissipation agent that must be considered when activating the nitinol for which the 40 ° C was chosen, which if we analyze it is within the range recommended by the manufacturer.

The constant power supply from 12V to 10 A is chosen, for the reason of power consumption and indefinite movement.

3.1 Actuator motion analysis

The actuator will be subjected to an external weight that is the pressure that will be exerted when submerged, since the robot will have an oscillatory displacement by means of the caudal fin must have the necessary force to break the barrier of movement in the water, movement tests were carried out with different weights with the angle of attack of 60 °, 90° and 120°.

It should be noted that the angles of the samples were taken from a set of 25 tests performed under ideal conditions and with previously demonstrated etching and activation parameters, the weights for the tests are 10g, 20g, 30g and 40g.

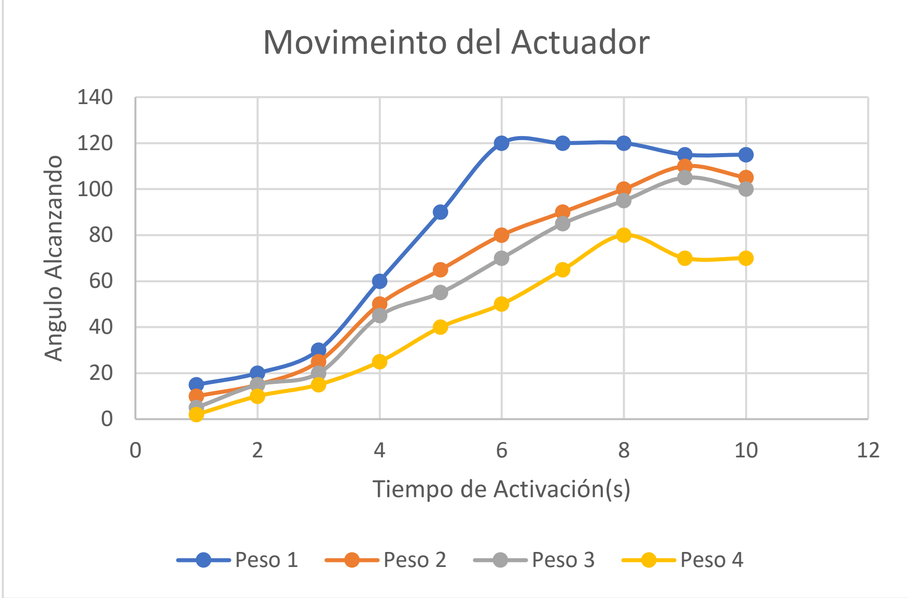

Figure 8. Movement according to a specified weight.

Figure 8 shows points that represent the relationship of time and final angle with the defined weight, the activation temperature previously selected with its respective source was considered, this is another proof of the use of a constant source of energy since it can take a certain time to reach its final angle and this implies a not so large energy consumption but that needs a period of Indefinite time, for this section the angle of attack of 90 ° is chosen, being the final result of the tests with the necessary force to reach its final displacement and with a considerable time.

3.2. Design and construction of the prototype

The prototype of bioinspired underwater robot has 3 fundamental parts the body, the pair of pectoral fins and the caudal fin, which were designed in SolidWorks and printed in 3D printing with TPU material. For the bioinspired design, several aspects were taken into account, such as: weight, stability, buoyancy, volume and shape of the different fins in conjunction with the body.

The body of the robot is shown in figure 9, in its design it has grooves in order to achieve good submersibility, in addition to a fixed dorsal fin that is centered on the back of the body in order to provide stability.

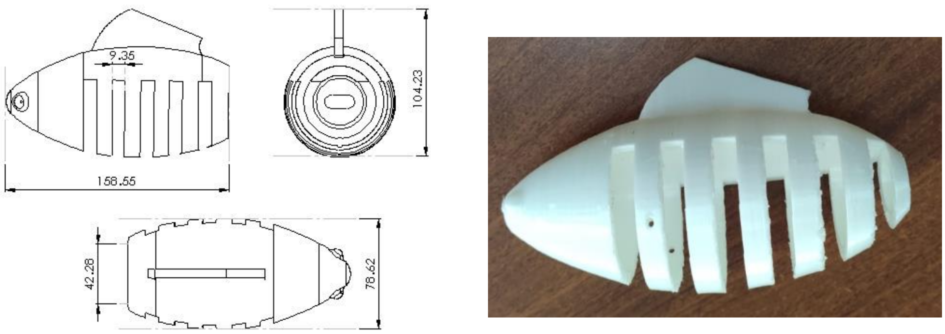

(a) (b)

Figure 9. Bioinspired robot body design: **(a)** Design in SolidWorks; **(b)** Implemented Body.

The caudal fin is formed of a caudal pendulum attached to a caudal fin thus forming a complete fin as shown in figure 10, for its design a mold with 3D printing was created, so that it is subsequently filled with antifungal silicone, said mold consists of 4 grooves where the unconventional actuators will be located rectangularly on the two opposite sides of the fin.

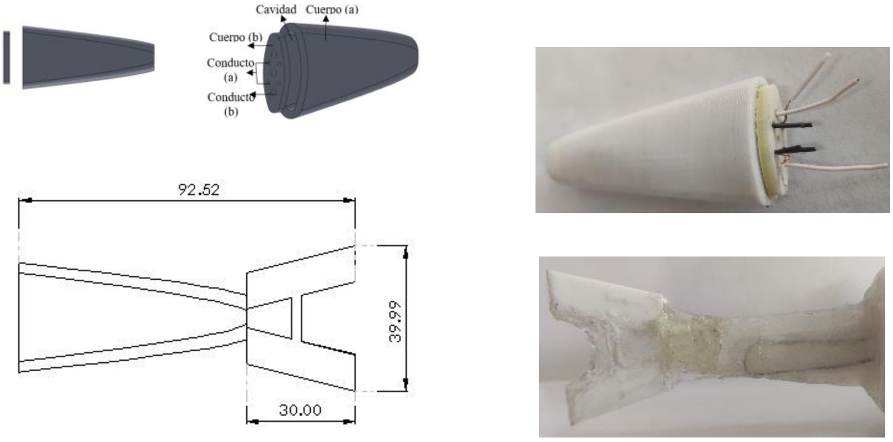

(a) (b)

Figure 10. Caudal fin design: **(a)** Design in SolidWorks; **(b)** Caudal fin implemented.

The pair of pectoral fins as shown in figure 11, seek to provide stability to the prototype in its design consists of two pieces with grooves where the unconventional actuators will be placed and later they will be covered by a thin layer of antifungal silicone used as insulation.

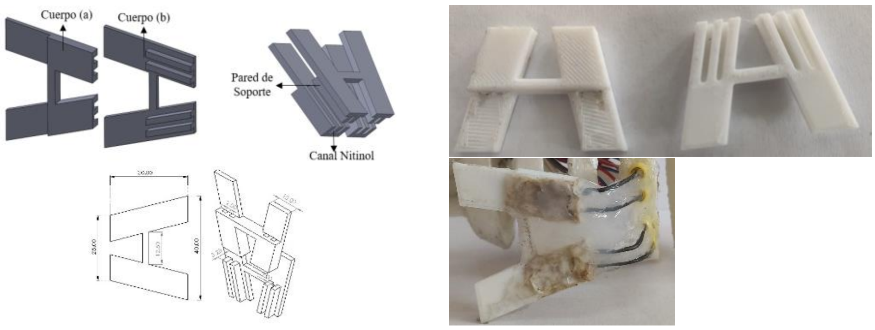

(a) **(b)**

Figure 11. Pectoral fin design: **(a)** Design in SolidWorks; **(b)** Pectoral fin implemented.

Once each of the parts has been designed separately, everything is joined together in order to have as a final result the bioinspired underwater robot as can be seen in figure 12, where the cables that will serve to control the metal-based actuators with shape memory come out.

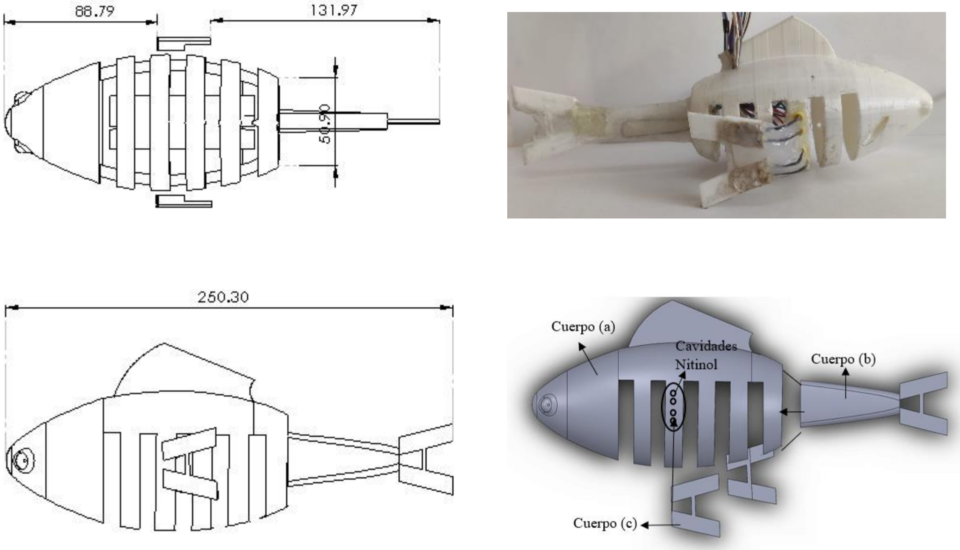

(a) (b)

Figure 12. Bioinspired robot prototype: **(a)** Design in SolidWorks; **(b)** Prototype implemented.

Once the bioinspired robot is ready, it is submerged in water and it is verified that the body is in balance and totally submerged to later make the different pieces to determine the displacement that our bioinspired robot performs, this study is carried out by using an inertial measurement unit sensor.

3.4. Trajectory of the bioinspired robot

3.4.1 Bioinspirado robot pocionaiento

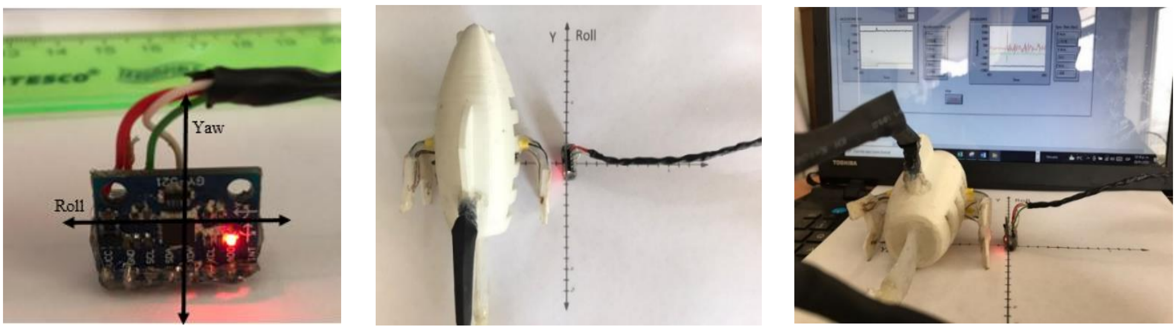

(**a**) (**b**) (c)

Figure 13. *Positioning of the* bioinspired robot: **(a)** Definition of axes and position of the IMU6050 sensor; **(b)** IMU 6050 sensor Positioning in the plane and with the bioinspired robot; **(c)** Test operation of IMU6050 sensor connection with LabVIEW Monitoring Interface.

Figures 13 show the positioning and initialization of the sensor since it depends on the position in which it is placed to obtain its initial data and its axes are also the test of the sensor with the connection of the graphical interface used the Lab-VIEW program for the collection of position data.

Table 1 Table simplified by points of the samples taken from the position of the bioinspired fish robot.

Table 1 shows the data obtained by the IMU 6050 sensor when activating the movement of the bioinspired fish, it is taken as a simplification of 7 points taken from the trajectory reached, these points are obtained from the 60 samples made and executed, the sensor sends data at the assigned points which in the first 3 points does not have a deviation away in the following points a deviation is observed which we interpret in a way as final absolute error.

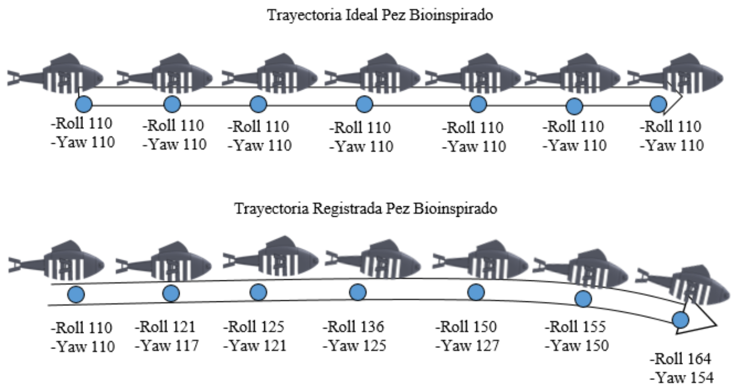

Figure 14. Trajectory of the bioinspired robot

Figure 14 shows the data obtained at 7 points of the trajectory of the Bioinspired

Sample	Position sent by the sensor				Position Obtained by drawing		Error				Error absolute	
	Expected values		Values obtained				Sensor		Sensor and drawing			
	Roll	Yaw	Roll	Yaw	Roll	Yaw	Roll	Yaw	Roll	Yaw	Roll	Yaw
1	110	110	110	110	110	110	0	0	0	0	0	0
2	110	110	121	117	118	113	11	7	8	3	3	4
3	110	110	125	121	127	123	15	11	17	13	2	2
4	110	110	136	125	128	124	26	15	18	14	8	1
5	110	110	150	127	153	124	40	17	43	14	3	3
6	110	110	155	150	150	142	45	40	40	32	5	8
7	110	110	164	154	156	149	54	44	46	39	8	5

Fish, which will be compared and its absolute error will be obtained, as two comparisons you have the expected value or initial data of the sensor and data taken in its trajectory, additional a plane was placed with degrees that was coupled to the aquarium, said plane are with marks of degrees in their Cartesian plane to be able to observe in a direct way the variation of trajectory in Roll and Yaw, with these data their absolute errors will be obtained and in the end a final absolute error between the two previous errors.

3.4.2 Activation sequence and angle of flexion of the caudal fin

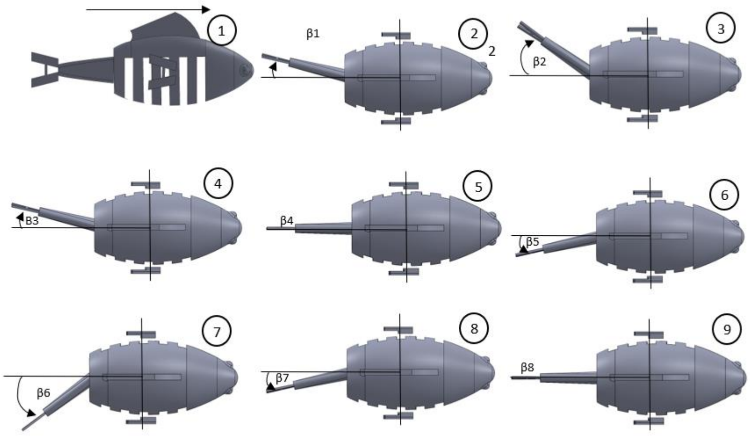

Figure 15. Caudal fin activation sequence.

Figure 15 shows the bending motion of the 1 mm nitinol wire embedded on the sides opposite the caudal fin. When heated by conducting a current on the copper wire, achieving austenite temperature, the actuator embedded on one side bends outwards causing the fin to move to that side, while the nitinol wire embedded on the outside side cools, the inner side is actuated which straightens the opposite wire and in turn performs the inward movement of the caudal fin, resulting in the propulsion of the robot. Movements to the right and left are observed with a certain angle of attack which was recorded at 90 °, when performing the tests in the water it was determined that the angle of attack decreases as the speed of the robot rises, the angle ß represents the displacement in the plane of the caudal fin where the activated begins in a ß1 at about 30 ° in relation to the plane, As it is activated, it takes different angles until it reaches the end point being ß2 with 60°, when the movement to the right is deactivated, the movement to the left is activated where it travels the same movement until it reaches a final ß6 with the same angle of 60°, thus obtaining a repetitive movement and generating the propulsion of the robot.

3.4.3 Activation sequence and angle of flexion of the pectoral fin

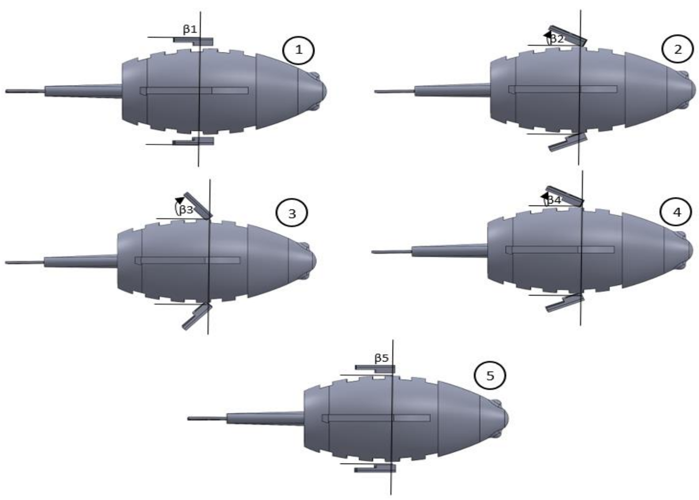

Figure 16. Activation sequence of the pectoral fin.

Figure 16 shows the bending movement of the nitinol wire of 1 mm embedded in the chest fin that allow stabilization or change of direction of the robot, in its design it consists of an angle of attack of 90 ° and when activated in a determined time according to the selected program travels different angles from a ß1 of 0 ° to reach its end point of a ß3 of 60 °, these steps are done cyclically with the difference that this fin can only reach from 0 ° to 60 ° for its structure and work, according to its programming performs the activation of the two fins to have a balanced swim, or one of the two fins independently according to the turn that is required.

3. Results

Figure 12 shows the bioinspired robot submerged in water, due to its body design and actuators embedded in its fins in order to sustain an oscillatory movement, which allows the bioinspired robot to move in an underwater environment, obtaining an etching temperature of $210 \pm 10°C$ and activation of$40°C$, for the actuator used in the caudal fin a 90° attack angle was used with an engraving and activation already specified, thus obtaining a propulsion of the robot by its tail with oscillatory movements, For the actuator used in the pectoral fin, an almost neutral stability and buoyancy and a two-dimensional displacement measured by the IMU 6050 sensor board or inertial meter which helps us to obtain data from the trajectory of the robot in terms of Yaw and Roll.

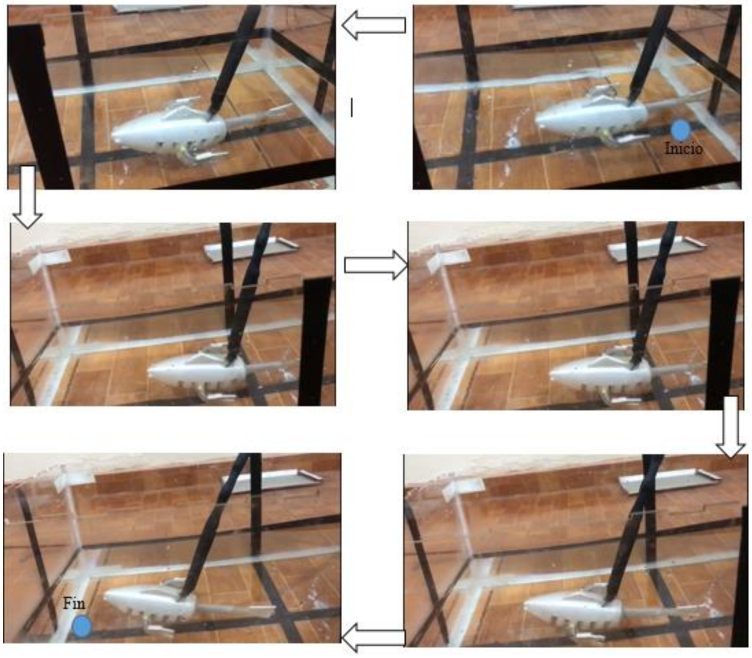

Figure 17. Test of the bioinspired robot in the underwater environment.

5. Conclusions

A bioinspired underwater robot was designed and implemented using metal-based actuators of shape memory for two-dimensional displacement in a controlled environment, where engraving data was obtained in the pectoral fin of in the caudal fin of and activation values for the caudal and pectoral fin and through an inertial measurement sensor we managed to obtain positioning data which were positions by points of the trajectory of the robot.$210 \pm 10°C210 \pm 10°C40 \pm 10°C$

Equipment and materials were selected according to the needs presented in the implementation of the bioinspired prototype, such as the TPU material and the antifungal silicone used for the implementation of the body and the different fins of the robot that thanks to its characteristics of flexibility and thermal resistance is suitable for the operation of the different actuators that were designed.

For the design of the bioinspired prototype, aspects such as hydrodynamic fusiform bioinspired shape, weight of 254.5g, caudal fin dimensions of 91.69mm long, 30mm of initial width and 40mm of final width, pectoral fin 30mm wide and 33mm long, and its body of 158.55mm long and 78.62mm wide, giving a total full body size of 249.37mm long and 92.5mm wide and almost neutral stability, to later work on the SolidWorks Software with which it allowed us to perform assembly, to obtain the model prior to its implementation.

The implementation of the robot was carried out using a power supply of 12V to 10 A for the actuators and a battery of 704V to 300mAh for the control, the control is placed outside the robot by means of an umbilical cord, and inside it a sensor card or inertial measurement unit was installed to obtain the data during navigation. The results yielded by the censor card were relatively imprecise due to their calibration, carried out the buoyancy and stability tests we obtained a totally submerged or almost neutral prototype.

References

[1] S. Guirado Gutiérrez, "Underwater LIBS Technology. Research, Development and Application to the Study of Submerged Archaeological Materials," 2015, Accessed: Jan. 30, 2022. [Online]. Available: https://dialnet.unirioja.es/servlet/tesis?codigo=103433&info=resumen&idioma=SPA

[2] R. Du, Z. Li, K. Youcef-Toumi, and P. Valdivia y Alvarado, Eds., "Robot Fish," 2015, doi: 10.1007/978-3-662-46870-8.

[3] H. A. Moreno, R. Saltarén, L. Puglisi, I. Carrera, P. Cárdenas, and C. Álvarez, "Underwater Robotics: Concepts, Elements, Modeling and Control," *Revista Iberoamericana de Automática e Informática industrial*, vol. 11, no. 1, pp. 3–19, 2014, doi: 10.1016/J.RIAI.2013.11.001.

[4] J. De, D. Rodriguez, G. Ferrol, and O. From, "GRUPO INNOVACIÓNS MARIÑAS DEPARTAMENTO DE CONSTRUCCIÓNS NAVAIS DOCTORAL THESIS DEVELOPMENT OF AN EXPERIMENTAL SYSTEM OF UNDULATING PROPULSION AND THE METHOD OF PREDICTING ITS BEHAVIOR BY CFD," 2010.

[5] S. F. Masoomi, S. Gutschmidt, X. Q. Chen, and M. Sellier, "The kinematics and dynamics of undulatory motion of a tuna-mimetic robot," *International Journal of Advanced Robotic Systems*, vol. 12, Jul. 2015, doi: 10.5772/60059.

[6] A. A. M. Faudzi, M. R. M. Razif, N. A. M. Nordin, E. Natarajan, and O. Yaakob, "A review on development of robotic fish," *Journal of Transport System Engineering*, vol. 1, no. 1, pp. 12–22, 2014.

[7] P. Duraisamy, R. Kumar Sidharthan, and M. Nagarajan Santhanakrishnan, "Design, Modeling, and Control of Biomimetic Fish Robot: A Review," *Journal of Bionic Engineering 2019 16:6*, vol. 16, no. 6, pp. 967–993, Dec. 2019, doi: 10.1007/S42235-019-0111-7.

[8] K. H. Low and A. Willy, "Development and initial investigation of NTU robotic fish with modular flexible fins," *IEEE International Conference on*

Mechatronics and Automation, ICMA 2005, pp. 958–963, 2005, doi: 10.1109/ICMA.2005.1626681.

[9] IEEE Robotics and Automation Society., *ICMA 2010 : 2010 IEEE International Conference on Mechatronics and Automation : August 4-7, 2010, Xi'an, China.* IEEE, 2010.

[10] Z. Chen and Y. Liu, "Design and Simulation Analysis of Bionic Devil Fish," in *2020 3rd International Conference on Mechatronics, Robotics and Automation, ICMRA 2020*, Oct. 2020, pp. 54–58. doi: 10.1109/ICMRA51221.2020.9398357.

[11] M. L. Muñoz, "Smart Materials: Shape Memory Alloys (SMA)," 2009. [Online]. Available: https://www.researchgate.net/publication/258108524

[12] G. v. Lauder and E. G. Drucker, "Morphology and experimental hydrodynamics of fish fin control surfaces," *IEEE Journal of Oceanic Engineering*, vol. 29, no. 3, pp. 556–571, Jul. 2004, doi: 10.1109/JOE.2004.833219.

[13] G. v Lauder, "Function of the Caudal Fin During Locomotion in Fishes: Kinematics, Flow Visualization, and Evolutionary Patterns 1," 2000. [Online]. Available: https://academic.oup.com/icb/article/40/1/101/2140072

[14] S. of the. FLOR, "FLOR, Silvia de la. 2005. Numerical simulation and experimental correlation of mechanical properties in shape memory alloys.," *Universitat Politècnica de Catalunya.* , 2005.

[15] F. R. Cabrera Aguayo, F. J. Santacruz Sulca, B. H. Bermeo Jiménez, and C. A. Orozco Cazco, "Design of bio-inspired fish robot powered by caudal fin with 1 GDL.," *Digital Science*, vol. 3, no. 3.3, pp. 345–355, Sep. 2019, doi: 10.33262/cienciadigital.v3i3.3.826.